PROCEEDINGS B

rspb.royalsocietypublishing.org

Research

Cite this article: Maynard DS, Leonard KE, Drake JM, Hall DW, Crowther TW, Bradford MA. 2015 Modelling the multidimensional niche by linking functional traits to competitive performance. *Proc. R. Soc. B* **282**: 20150516. http://dx.doi.org/10.1098/rspb.2015.0516

Received: 4 March 2015
Accepted: 2 June 2015

Subject Areas:
ecology, theoretical biology, microbiology

Keywords:
competition, Hutchinsonian niche, performance, realized niche, *Saccharomyces cerevisiae*, traits

Author for correspondence:
Daniel S. Maynard
e-mail: daniel.maynard@yale.edu

Electronic supplementary material is available at http://dx.doi.org/10.1098/rspb.2015.0516 or via http://rspb.royalsocietypublishing.org.

THE ROYAL SOCIETY PUBLISHING

Modelling the multidimensional niche by linking functional traits to competitive performance

Daniel S. Maynard[1], Kenneth E. Leonard[2], John M. Drake[2], David W. Hall[3], Thomas W. Crowther[1] and Mark A. Bradford[1]

[1]School of Forestry and Environmental Studies, Yale University, 370 Prospect Street, New Haven, CT 06511, USA
[2]Odum School of Ecology, and [3]Department of Genetics, University of Georgia, Athens, GA 30602, USA

Linking competitive outcomes to environmental conditions is necessary for understanding species' distributions and responses to environmental change. Despite this importance, generalizable approaches for predicting competitive outcomes across abiotic gradients are lacking, driven largely by the highly complex and context-dependent nature of biotic interactions. Here, we present and empirically test a novel niche model that uses functional traits to model the niche space of organisms and predict competitive outcomes of co-occurring populations across multiple resource gradients. The model makes no assumptions about the underlying mode of competition and instead applies to those settings where relative competitive ability across environments correlates with a quantifiable performance metric. To test the model, a series of controlled microcosm experiments were conducted using genetically related strains of a widespread microbe. The model identified trait microevolution and performance differences among strains, with the predicted competitive ability of each organism mapped across a two-dimensional carbon and nitrogen resource space. Areas of coexistence and competitive dominance between strains were identified, and the predicted competitive outcomes were validated in approximately 95% of the pairings. By linking trait variation to competitive ability, our work demonstrates a generalizable approach for predicting and modelling competitive outcomes across changing environmental contexts.

1. Introduction

Competition is a dominant structuring force in community assembly, yet it is often difficult to predict how competitive outcomes change along environmental gradients. Understanding these interactions is essential for accurately predicting species' realized niche spaces and geographical distributions [1–3]. Organisms compete through a wide range of mechanisms and strategies, with most models of competition applying only to a specific organism or to a specific mode of competition. Alternatively, functional traits—which connect performance to abiotic and biotic conditions [4]—offer a separate approach for linking competitive ability and environmental variables. Trait-based models can quantify organismal performance and competitive ability along gradients, and in turn, use these relationships to predict competitive outcomes under novel environmental conditions [5,6]. Although correlations between trait values and biotic outcomes have been used to infer competitive ability from individual trait expression [7–10], rarely do such approaches provide a framework for predicting competitive outcomes across study systems. The inclusion of biotic interactions in niche and species distribution models is thus contingent on the development of generalizable, quantitative techniques for directly linking trait expression to competitive outcomes across resource gradients [6].

A challenge for any niche model is its ability to disentangle biotic and abiotic determinants of individual performance. Correlative and statistical

trait-based models can simultaneously capture the combined effects of multiple environmental variables without requiring direct measurements of fitness or fundamental niche spaces [11–14]. These models have proven invaluable for inferring species distributions from trait distributions, but correlative approaches are limited in their capacity to identify causal relationships that are necessary for extrapolating to novel communities or environments [13,15–17]. Conversely, mechanistic models rely on prior knowledge about the processes that link fitness to environmental conditions, allowing them to directly incorporate biotic and abiotic change [12,16,17]. Since these models assume a single, known competitive mechanism, they do not apply to those systems where the mode of competition is unknown or takes a form other than what is assumed. For example, resource-ratio models (e.g. 'Tilman's R*'; [18–20]) mechanistically incorporate biotic interactions by assuming that species compete by 'drawing down' resources and maintaining positive growth at lower resource levels. Although this form of resource competition has been shown experimentally in some systems, a large body of evidence suggests that it is not a universal competitive mechanism, limiting the usefulness of this model in many settings (reviewed in [21]). As an alternative to these approaches, recent trait frameworks have proposed the usefulness of trait-based 'performance metrics' to approximate the relative fitness and competitive ability of organisms along environmental gradients [5,6]. In theory, such an approach can be used to identify competitive outcomes under different environmental conditions regardless of the competitive mechanism, provided that the performance metric is a reasonable indicator of competitive ability.

Here, we present and empirically test a novel competition model that builds on existing trait-based frameworks by using functional traits to predict competitive outcomes of co-occurring populations across multiple resource and/or abiotic gradients. In contrast to existing trait-based species distribution models, the proposed model quantifies the performance of organisms in the absence of competition (i.e. the fundamental niche) and uses the results to predict the outcomes of biotic interactions (i.e. the realized niche). First, we present the mathematical basis of the model and show how it estimates performance of a single population. Second, we test the model by characterizing the performance of six genetically related yeast strains in laboratory microcosms. The competitive ability of each strain is displayed as a third dimension across this resource space, thus directly modelling a Hutchinsonian '*n*-dimensional hypervolume' along two resource gradients [22]. Areas of coexistence and competitive exclusion are identified visually using differential performance plots, and quantitatively, by calculating the exact difference in performance between populations at a given resource supply. Lastly, these model-based predictions of competitive dominance and coexistence are tested across a range of carbon and nitrogen nutrient concentrations.

The model requires estimating only three traits per population. It does not depend on the extent to which a species can deplete a resource, nor does it make any assumptions about the mechanisms by which populations compete. Rather, it applies to those settings where competitive ability along resource gradients is directly proportional to the expression of a competitive trait or performance metric. The model is thus particularly suited for situations when resource supply rates or initial population conditions cannot reliably be estimated or projected through time (as is likely the case in many ecosystems) or when species compete through interference or apparent competition.

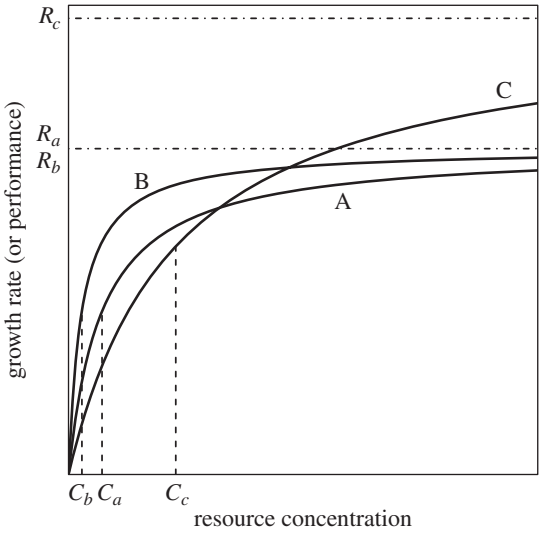

Figure 1. The model uses the Monod function to relate performance to resource availability. The performance curves of three hypothetical populations (*A*, *B*, *C*) are shown here, with each curve determined by that population's maximum intrinsic growth rate (R_x, horizontal dashed lines) and its half-saturation constant (C_x, vertical dashed lines; where growth rate is equal to 1/2 R_x). The competitive dominance of a population across the resource gradient can be owing either to a low half-saturation constant (i.e. high affinity for that resource) or a high maximum growth rate. For example, populations *A* and *B* have the same maximum intrinsic growth rate ($R_a = R_b$), but *B* has a higher affinity for the resource ($C_b < C_a$), making it more competitive than *A* at all resource concentrations. Population *C* has a high maximum intrinsic growth rate but a low resource affinity (high C_C), making it competitively dominant over *A* and *B* only at high resource concentrations.

2. Material and methods

(a) Trait-based competition model

The model presented here (termed the 'Leonard Model') uses the Monod function to link species performance to environmental conditions [23]. The Monod function was originally formulated to link realized intrinsic growth rate, *R*, to resource concentration by

$$R = R_K \frac{S}{C_S + S}, \tag{2.1}$$

where R_K is maximum growth rate of the population, *S* is the instantaneous resource supply concentration and C_S is the resource supply concentration required to achieve one-half R_K, termed the 'half-saturation constant' (figure 1).

When a population is dual-limited by multiple resources its growth can be regarded as following von Liebig's 'Law of the Minimum' [18,24]. Using Monod's notation for two resources, *A* and *B*, the growth rate is determined by whichever resource is most limiting:

$$R_{A,B} = \min\left[R_{KA}\frac{A}{C_A + A}, R_{KB}\frac{B}{C_B + B}\right]. \tag{2.2}$$

Since the maximum intrinsic growth rate is a fundamental trait of the organism, it follows that $R_{KA} = R_{KB} = R_K$, and thus:

$$R = R_K \min\left[\frac{A}{C_A + A}, \frac{B}{C_B + B}\right]. \tag{2.3}$$

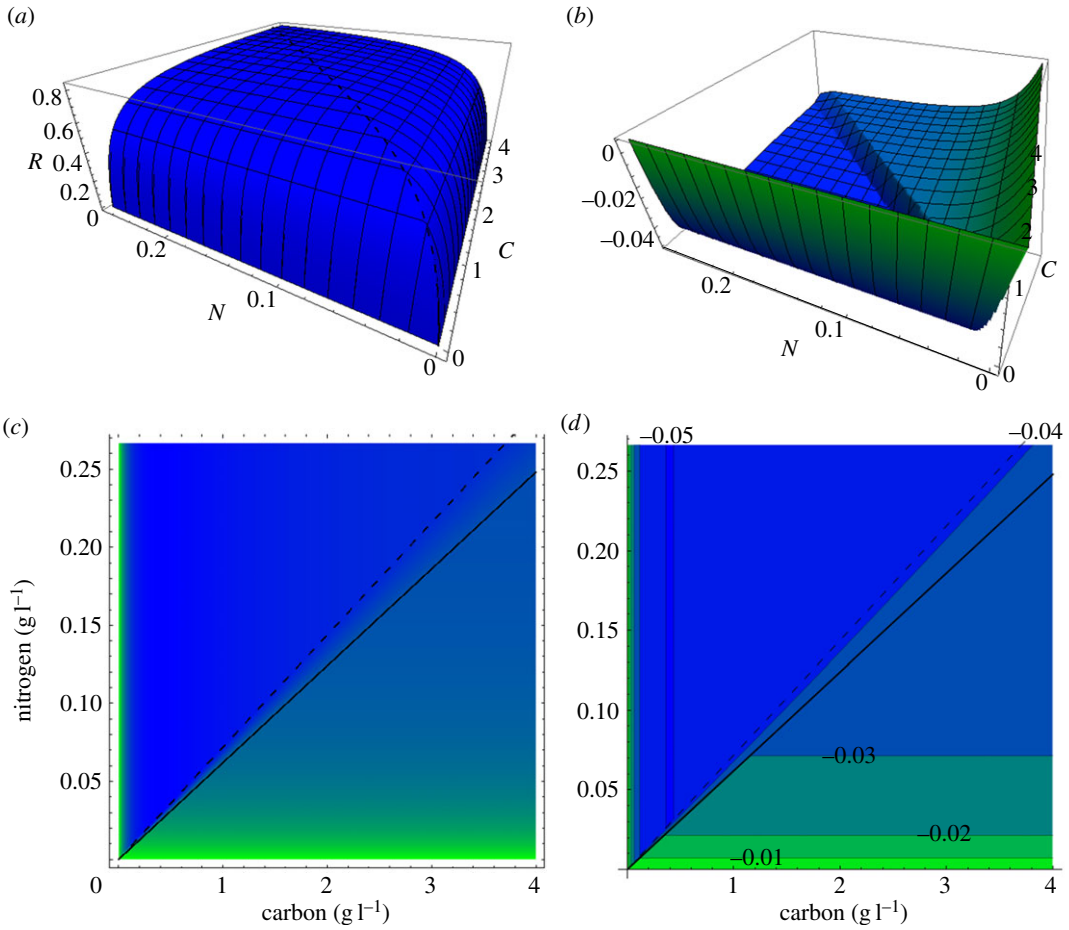

Figure 2. Growth and differential response surfaces for the two original wild-type isogenic strains, P1 and P2, across a carbon and nitrogen gradient. (*a*) The overlaid growth response for each species, with the response surface of P2 (blue) fully obscuring the response surface for P1 (yellow) in this example (but see figure 3). (*b*) The plot of ΔR, denoting areas of competitive dominance or coexistence (shaded green); there are no yellow areas because nowhere does P1 outcompete P2. (*c*) The flat-shaded contour map, showing a continuous transition between coexistence and competitive dominance. (*d*) The contour-stepped map, with discrete ΔR cut-points to facilitate prediction of coexistence and competitive dominance. Despite a higher carbon and nitrogen affinity by P1, the growth rate of P1 was predicted to be lower than P2 at all resource concentrations owing to a significantly higher R_K value for P2 (table 1). Coexistence was predicted only at low nitrogen concentrations.

A plot of R as a function of the three response traits—C_A, C_B and R_K—illustrates the population's performance across a resource space, with $R > 0$ outlining the organism's fundamental niche space. The ratio of the half-saturation constants, C_A/C_B, gives the slope of the optimum proportion line, as described by Tilman [18], and is equivalent to the dual-limitation ratio [25] or the stoichiometric optimum.

The difference in population growth rates between two populations, Y and Z (with corresponding maximum growth rates and half-saturation constants), can be calculated as:

$$\Delta R = R_{KY} \min\left[\frac{A}{C_{A,Y} + A}, \frac{B}{C_{B,Y} + B}\right] - R_{KZ} \min\left[\frac{A}{C_{A,Z} + A}, \frac{B}{C_{B,Z} + B}\right]. \quad (2.4)$$

In settings where growth rate is a meaningful surrogate for competitive ability, the metric ΔR can be used to distinguish between competitive exclusion and coexistence among co-occurring populations. By plotting this growth difference as a third dimension across the resource gradient, these areas of competitive exclusion and coexistence are visualized (e.g. figure 2).

Although equation (2.4) is formulated in terms of organismal growth rate, the Leonard Model is not restricted to those settings where competitive ability correlates with growth, nor is it restricted to those settings where competitive ability is dictated solely by resource concentrations. Indeed, the Monod function—selected here for its simplicity and its previous use in various theoretical and applied competition studies [25–27]—is analogous to other common ecological and biogeochemical functional forms, such as the Holling Type II functional response curve [28] and the Michaelis–Menten equation for enzyme kinetics [29]. For generalizability and simplicity, however, we refer to 'growth rate' as the relevant performance metric and 'resource availability' as the relevant environmental gradient throughout. Furthermore, to test the model empirically, the experimental microcosms were selected and constructed such that resource capture was the dominant competitive mechanism, meaning that difference in growth rate across nutrient concentrations was likely to correlate with competitive ability.

(b) Study populations

A series of controlled microcosm experiments were conducted to test the model, using the widely distributed unicellular yeast *Saccharomyces cerevisiae* (Meyen ex E.C. Hansen). Two isogenic strains were isolated from wild-type populations in Kumeu River, Auckland, New Zealand; each strain was less than 50 generations removed from the wild population. From these two original strains (denoted P1 and P2), we derived an additional four strains using two different approaches. First, we generated a version of each strain carrying a genomic, antibiotic-resistance gene that allowed the strain to grow on media amended by the antibiotic nourseothricin (see the electronic supplementary

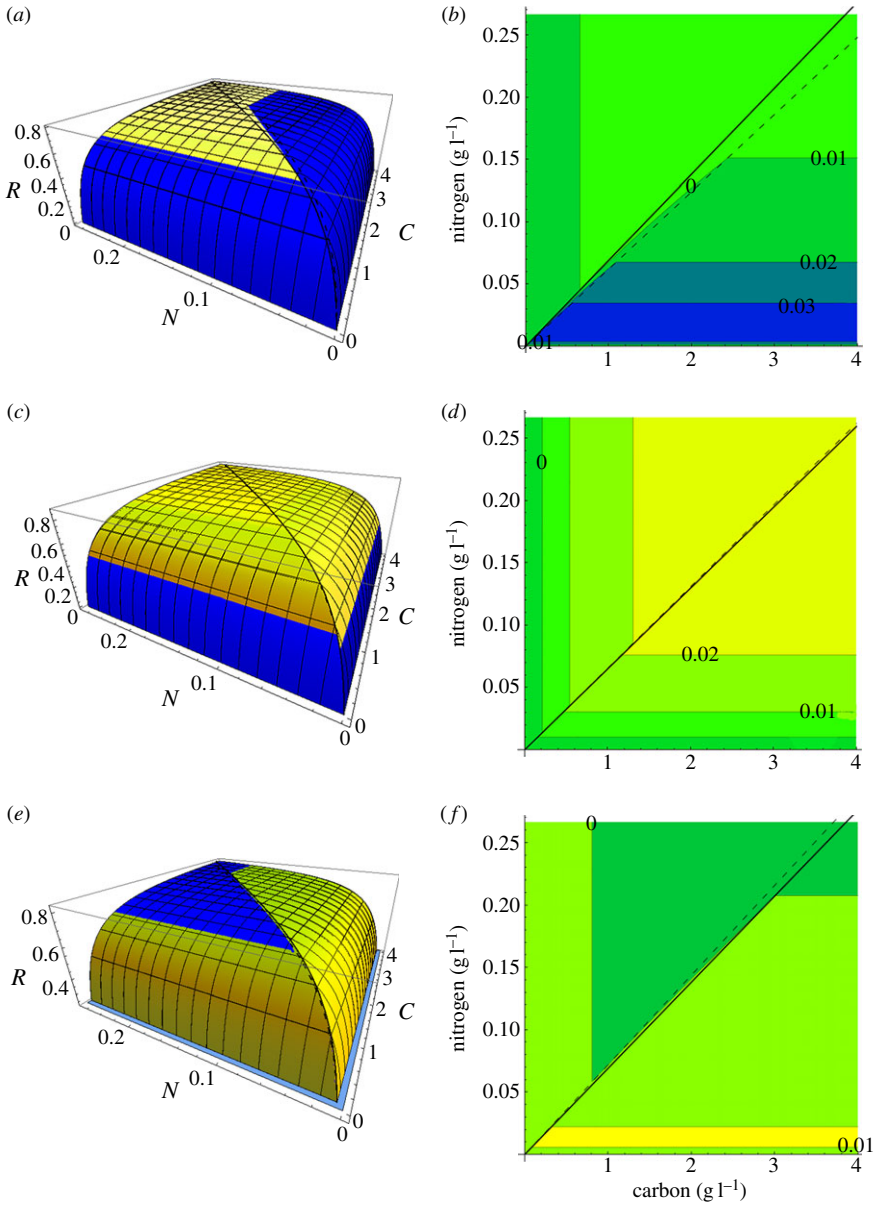

Figure 3. Growth surfaces and contour-stepped maps for the antibiotic-resistant strains and the descendent strains. (*a*,*b*) Though $P1^R$ (yellow) had higher performance at moderate-to-high availabilities of carbon and N, ΔR remained less than 0.01 throughout most of this region, indicating coexistence. Higher growth rates by P1 (blue) at low nitrogen concentrations indicated likely competitive dominance by P1 when nitrogen was limiting. (*c*,*d*) A higher R_K value for $P2^R$ (yellow) relative to P2 (blue) led to significantly increased growth rates at most resources concentrations, with predicted competitive dominance everywhere but at moderately low carbon and nitrogen availability. (*e*,*f*) The Low-N strain (yellow) was predicted to be dominant over the Low-C strain (blue) at low nitrogen concentrations, but otherwise showing coexistence (green). The Low-C and Low-N strains both exhibited competitive dominance over their ancestor strains (not shown; see electronic supplementary material, figure S1) everywhere except at very low nitrogen concentrations.

material). Since the populations could not otherwise be identified, this approach enabled us to assess competitive outcomes between an antibiotic-resistant strain and a non-resistant strain by measuring relative growth on antibiotic-amended culturing plates relative to regular plates.

Second, we adapted eight replicates of P1 to severe carbon limitation (a carbon : nitrogen ratio 0.076-times the optimum) and eight replicates to severe nitrogen limitation (a carbon : nitrogen ratio 38.5-times the optimum) for more than 250 generations. We then used in subsequent experiments the replicate strain that grew best in severe carbon limitation (denoted 'Low-C') and the replicate strain that grew best in severe nitrogen limitation (denoted 'Low-N'). The goal was to derive closely related isolates with altered performance from their ancestors across the resource gradient. As such, we did not attempt to identify whether resulting changes in fitness occurred through nutrient limitation and/or adaptation to general microcosm conditions. These two approaches—gene alteration and microevolution—led to six genetically related yeast strains: two original strains (P1 and P2); two antibiotic-resistant, descendant strains ($P1^R$ and $P2^R$); one strain adapted to severe carbon limitation ('Low-C') and one strain adapted to severe nitrogen limitation ('Low-N').

(c) Measuring response traits and performance

All experiments were conducted using chemostats with constant nutrient-input concentrations and aerobic conditions. Chemostats are a common approach to studying fitness and performance among genetically related microbial populations, often in relation to microevolution and environmental adaptation [25,27,30,31]. The advantage of the chemostat design is that it permits direct testing of the model assumptions because populations are maintained in log-phase growth, the rate of which is strictly controlled by the nutrient concentrations of the inflow media. This

Table 1. Model-derived growth trait parameters for all *Saccharomyces cerevisiae* yeast strains. R_K, the maximum capable intrinsic growth rate; C_C the carbon half-saturation constant; C_N the nitrogen half-saturation constant; C : N: the ratio of half-saturation constants (equal to the 'dual-limiting ratio' or the slope of the optimum proportion line). R^2_{adj}: the overall model fit of R_K, C_N and C_C. Standard errors and 95% CIs for R_K, C_C and C_N were estimated during model fitting; standard errors and 95% CIs for C : N were estimated via Monte Carlo simulation (see §2e). $P1^R$ and $P2^R$ are the antibiotic-resistant strains of P1 and P2, respectively. Low-N and Low-C are descendent populations of P1, grown under limiting nitrogen and carbon concentrations, respectively.

strain	$R_K \pm$ s.e.	95% CI	$C_C \pm$ s.e.	95% CI	$C_N \pm$ s.e.	95% CI	C : N ± s.e.	95% CI	R^2_{adj}
P1	0.83 ± 0.05	(0.72, 0.95)	0.210 ± 0.04	(0.13, 0.29)	0.0130 ± 0.002	(0.009, 0.017)	16.2 ± 4.3	(15.9, 16.4)	0.95
$P1^R$	0.85 ± 0.04	(0.76, 0.93)	0.223 ± 0.03	(0.16, 0.29)	0.0154 ± 0.002	(0.012, 0.019)	14.5 ± 2.7	(14.3, 14.7)	0.97
P2	0.90 ± 0.04	(0.82, 0.97)	0.216 ± 0.02	(0.17, 0.26)	0.0142 ± 0.001	(0.011, 0.017)	15.2 ± 2.4	(15.1, 15.4)	0.98
$P2^R$	0.93 ± 0.05	(0.83, 1.02)	0.232 ± 0.03	(0.17, 0.29)	0.0150 ± 0.002	(0.012, 0.019)	15.5 ± 2.7	(15.3, 15.6)	0.97
Low-N	0.87 ± 0.04	(0.79, 0.95)	0.181 ± 0.02	(0.13, 0.23)	0.0125 ± 0.001	(0.010, 0.016)	14.5 ± 2.7	(14.3, 14.7)	0.98
Low-C	0.87 ± 0.04	(0.78, 0.96)	0.184 ± 0.03	(0.13, 0.24)	0.0133 ± 0.002	(0.010, 0.017)	13.8 ± 2.8	(13.7, 14.0)	0.97

approach was motivated by early applied research based on resource-ratio theory of competition, where organisms were grown in greenhouses or microcosms under tightly controlled resource conditions (e.g. Tilman [26], [32]). The use of chemostats also ensured that resource capture was the dominant competitive mechanism and thus that 'growth rate' would be a reliable performance metric [27,30].

To estimate the growth response traits (C_A, C_B and R_K) and to model the performance curve (R) across the full resource space, each of the six strains was grown under eight different carbon and nitrogen supply rates, each replicated four times. Initial tests showed that resource concentrations of $1.5\ g\ C\ l^{-1}$ and $0.064\ g\ N\ l^{-1}$ were non-limiting for both parental strains, and each of these was used as a base concentration while the other nutrient was varied across four concentrations (electronic supplementary material, table S1). The strains were grown under each of the eight resulting concentrations for 25 generations at a 4.69 h ($0.213\ h^{-1}$) culture turnover time, and the ending biomass was used to estimate growth rate. Biomass was determined by extracting a known volume of the culture, collecting the cells and weighing them (see the electronic supplementary material for full methods).

(d) Measuring competitive outcomes

To test the ability of our model to predict areas of competitive dominance and coexistence, we performed 28 experimental competitions using the chemostat system. It was not possible to determine the outcomes of competitive interactions between two antibiotic-resistant or two non-resistant strains, so each pairing involved one resistant strain and one non-resistant strain. To prevent the complication of adaptive evolution occurring across many generations, competition was performed for 25 generations. An absolute value of 0.01 for ΔR was chosen as the threshold between 'competitive dominance' and 'coexistence'. When $\Delta R > 0.01$, the weaker strain would be expected to decrease in relative abundance from 50% to less than 44% over 25 generations, permitting us to reliably distinguish competitive outcomes in chemostat cultures. Furthermore, we anticipated that a fitness difference of less than 0.01 would lead to stochastic fluctuations in relative strain abundances, allowing the weaker competitor to maintain relatively high abundances and potentially even exclude the stronger competitor in some instances [33].

A variety of fungal pairings and resource concentrations were selected such that ΔR was greater than 0.01 in some pairings, increasing the likelihood of competitive dominance of one strain, and less than 0.01 in others, indicating likely coexistence. Each competitive pairing consisted of the two strains grown in the same chemostat culture flask for 25 generations at a 4.69 h culture turnover time. The resulting cultures were diluted to approximately 2×10^4 cells ml^{-1}, and 10 µl of this dilution were plated onto four yeast extract-peptone-dextrose (YPD plates and equally distributed across the surface by gently rotating the plates. Nourseothricin was added to two of these four at $100\ \mu g\ l^{-1}$ to prevent growth of the non-resistant strains (denoted 'antibiotic plates'). All plates were incubated for 24 h at 30°C and examined for colony growth. If fewer than 50 colonies were identified on a plate then all replicate plates for that pairing were incubated for an additional 24 h.

For each pairing, the competitive outcome was estimated by comparing the growth on the antibiotic plates with the growth on the standard plates. Each plate was covered with a randomly oriented counting grid, made of a 10 cm diameter opaque disc with seven randomly located windows, each measuring 1.25 × 1.25 cm. The number of colony forming units (CFUs) in each window was counted, excluding the windows with the largest and smallest numbers of yeast colonies. Since growth on the antibiotic plates reflected just the antibiotic-resistant strains, the ratio 'CFUs on antibiotic plates/CFUs on standard plates' was used to quantify the relative proportion of the antibiotic-resistant strain in the culture. A ratio of approximately 0.5 indicated equal

colony growth between the two strains, whereas a proportion that was significantly different from 0.5 indicated dominance of one of the competitors.

The 28 competitive pairings were split into an initial run of 12 pairings and a subsequent run of 16 pairings. The initial run was conducted with eight replicates per pairing and a precise count of CFUs on the plates to allow us to determine the degree of precision necessary to identify competitive dominance between two strains. These 12 pairings showed that 25 generations and a visual estimation of CFUs were sufficient to determine competitive dominance. The subsequent 16 competitive pairings were therefore conducted across a wide range of resource concentrations with two replicates per pair, and the proportion of CFUs on the plate visually estimated rather than counted.

(e) Statistical methods

Using growth rate measurements, we simultaneously estimated the three traits (R_K, C_N and C_C) for each isolate using a curve-fitting algorithm designed and implemented in *Mathematica*® (Wolfram Research 2013). Parameters were estimated via the function *NonlinearModelFit*, which by default uses the Levenberg–Marquardt method to minimize the sum-of-squares of the deviations between the observed and predicted data. The model output gives an ANOVA table for the overall model fit, along with standard errors, confidence intervals (95%), *t*-statistics and *p*-values for each fitted parameter (the full algorithm is available in the electronic supplementary material). We obtained summary statistics of the carbon : nitrogen (C : N) ratios (i.e. the optimum proportion lines) by Monte Carlo simulation. Specifically, for both C_C and C_N, 1000 samples were randomly drawn assuming a normal distribution with mean and standard deviation given by the fitted parameter estimates. The C : N ratios of each of these 1000 paired samples were calculated, along with the mean, variance and 95% confidence intervals.

In the initial run of 12 competitive pairings, the outcome was assessed by testing if the mean proportion of CFUs across the 8 replicates was statistically different from 0.5. For each pairing, the proportion was assumed to follow a standard normal distribution with unknown variance. A Student's *t*-test was used to test the null hypotheses that the mean proportion of antibiotic-resistant colonies at the end of the competition was 50% (i.e. that neither strain was dominant), and corresponding *p*-values and 95% CIs were calculated. The quantitative outcome (win, lose, uncertain) was determined based on whether the 95% CI was greater than, less than or included 0.5.

In the subsequent 16 pairings, the use of two replicates precluded statistical testing but still allowed for identification of the dominant strain. The proportion of CFUs on the antibiotic plates was scored as 'less than', 'greater than' or 'approximately equal' to 50% of the growth on the standard plates. If the number of CFUs on the antibiotic plate was less than half of the total number of CFUs on the standard plate, then the outcome was scored as a 'loss' for the antibiotic-resistant strain; conversely, if the number of antibiotic CFUs was greater than half the number of CFUs on the standard plate, the outcome was scored as a 'win' for the antibiotic-resistant strain. If the two replicate plates for a pairing showed contrasting results or if the estimated relative proportion was close to 0.5 then the outcome was scored as a 'draw' (indicating coexistence).

3. Results

(a) Model-based niche spaces and functional traits

The model accounted for over 95% of the variation in growth across all strains ($R^2_{adj} > 0.95$ for all strains; table 1) across both nutrient gradients. There were clear differences in growth parameters of the two wild-type strains: P1 had a 7% lower R_K than P2 and a higher affinity for carbon and nitrogen uptake (represented by the lower half-saturation constants for both carbon and nitrogen). These differences translated to a lower optimal C : N ratio (i.e. higher slope of the optimum proportion line) for P2 relative to P1, with corresponding differences in growth rates between the two strains (figure 2). Based on relative growth rate, P2 would be expected to outcompete P1 at all resource concentrations, with competitive dominance subject to stochastic uncertainty at low carbon and nitrogen values (figure 2*d*).

Antibiotic resistance also altered growth parameters, leading to higher estimated values for R_K, C_N and C_C in antibiotic-resistant strains relative to their parent strains (table 1). The higher C_N and C_C values for $P1^R$ and $P2^R$ led to lower predicted growth rates than P1 and P2, respectively, at low carbon and nitrogen concentrations (figure 3*a–d*). The higher R_K values of $P1^R$ and $P2^R$ led to higher predicted growth rates at higher carbon and nitrogen supply rates. P1 was predicted to remain the competitively dominant strain at low nitrogen values, but everywhere else competitive dominance was predicted to be subject to stochastic effects. $P2^R$ was predicted to be dominant at moderate-to-high carbon and nitrogen supply rates, with P2 remaining stochastically dominant at low concentrations (figure 3*d*).

Both of the nutrient limitation regimes led to distinct microevolutionary changes in growth trait parameters. Low-N and Low-C strains both increased their maximum capable growth response trait, R_K, by 5% (from 0.83 to 0.87; table 1). The Low-C derived strain had a reduced half-saturation C-response trait parameter, C_C, and an increased half-saturation N-response trait parameter, C_N. These two shifts combined to give a reduced optimum C : N ratio relative to P1, which is consistent with adaptation to low carbon. However, the Low-N derived strain had a lower half-saturation carbon response trait parameter than the Low-C descendant (0.181 ± 0.02 for Low-N versus 0.184 ± 0.03 for Low-C). The Low-N descendent also reduced its half-saturation N-response trait parameter, and showed a higher optimal C : N ratio (14.5, 95% CI = [14.3, 14.7]) than the Low-C descendant (13.8, 95% CI = [13.7, 14.0]). Both descendent strains had a statistically reduced C : N ratio from the ancestor strain, P1 (16.2, 95% CI = [15.9, 16.4]). These results may indicate adaptation to chemostat conditions and/or nutrient limitations.

Despite the different resource regimes under which Low-N and Low-C isolates adapted, their predicted growth rates were similar throughout the plotted carbon and nitrogen range (figure 3*e,f*). Growth plots show that Low-C has higher predicted growth rates than Low-N only at moderate carbon concentrations and relatively low C : N ratios. However, the maximum difference in realized growth response of the two descendants is only 0.0113 throughout the plotted range, suggesting that the outcome of competition between them is highly subject to stochastic effects in all environments.

(b) Competitive outcomes

Model-based estimates of growth rate were strong predictors of competitive dominance across the two resource gradients (figure 4; electronic supplementary material, tables S2 and S3). In the 12 initial pairings with high replication, the model correctly predicted the outcome in all cases. Of the subsequent 16

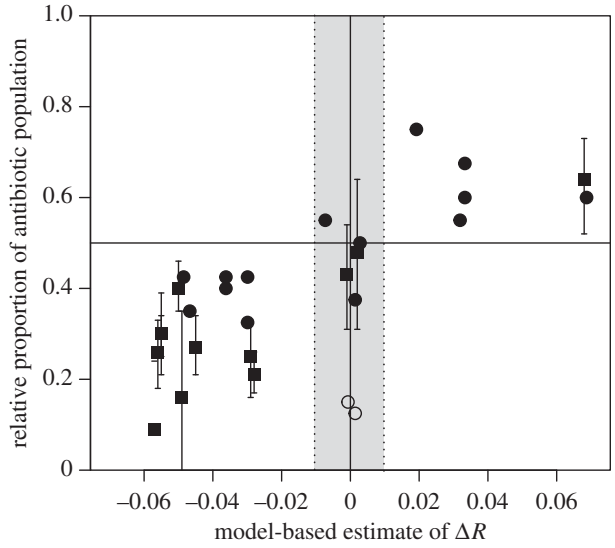

Figure 4. The results of the 28 competitive trials, with the relative proportion of the antibiotic-resistant strain in the final culture plotted against the model-based estimates of ΔR (antibiotic-resistant strain minus non-resistant strain). Squares indicate the initial set of competitive trials conducted with eight replicates each, with vertical bars corresponding to the 95% CI for each proportion. Circles indicate the subsequent set of trials conducted with two replicates each and a visual estimation of CFU proportion. The shaded region corresponds to $\Delta R < 0.01$, indicating likely coexistence between the pairs of isolates. Solid symbols denote trials where the outcomes were correctly predicted and empty symbols denote incorrect predictions.

competitive pairings, the model correctly predicted the outcome in 14 cases, with the remaining two pairings showing a consistent winner, despite ΔR being less than 0.01.

P2 and $P2^R$ were correctly predicted to be competitively dominant over P1 and $P1^R$ across all carbon and nitrogen concentrations (electronic supplementary material, table S3). P2 showed a slight competitive advantage over $P2^R$ at low carbon concentrations whereas the model suggested stochastic uncertainty (two empty circles, figure 4). P1 was correctly predicted to be competitively dominant over $P1^R$ at low nitrogen concentrations, with otherwise uncertain dominance. The higher R_K and lower C_C and C_N values for Low-N and Low-C relative to $P1^R$ led to complete competitive dominance at all carbon and nitrogen concentrations (electronic supplementary material, table S2). Indeed, the modelled growth rates of these descendants are greater than the ancestor at all resource concentrations, allowing for potential coexistence or stochastic outcomes only at extremely low resource concentrations but nowhere allowing for competitive dominance by the ancestor strains (electronic supplementary material, figure S1).

4. Discussion

The Leonard Model presented here quantifies response traits of different populations and then uses these traits to predict and visualize competitive outcomes along multiple environmental resource gradients. The experimental competitions suggested that the model was a robust predictor of competitive outcomes, demonstrating the potential to estimate realized niche spaces from organismal performance. The model therefore avoids some of the limitations of resource-ratio theory and correlative niche models, such as practical difficulties in estimating consumption and supply rates or difficulties accounting for colinearity among observed biotic and abiotic variables [15,21]. By alleviating these limitations, the model provides a generalizable means of predicting competitive outcomes regardless of the underlying competitive mechanism.

As with other mechanistic and correlative models [11,13,14,18], a fundamental assumption in the Leonard Model is that an organism whose traits are best adapted to that environment will be most competitive. This is exemplified by the dominance of the Low-N strain at low nitrogen concentrations. To link traits to fitness, the Leonard Model requires independent measurements of organismal performance across resource space, assayed in controlled conditions in the absence of competition (similar to Tilman's R* approach [18]). In contrast to this mechanistic modelling approach, correlative trait-based models rely on observational measurements of trait and/or species distributions, assayed in natural (or minimally manipulated) field conditions. The challenge in using observational data is how best to infer potential distributions under changing environmental conditions, such as when a competitor goes locally extinct. By directly modelling the fundamental niche space and quantifying relative competitive ability across this space, the Leonard Model is specifically designed to make such inferences. The remaining challenge with our approach, however, is how best to incorporate the necessary levels of real-world complexity so that the experimental system reflects the dominant forces structuring an organism's realized niche.

In natural communities, growth and survival are simultaneously governed by multiple biotic and abiotic factors, all of which are essential for structuring the realized niche. Our research is thus intended to serve as a first step towards linking biotic outcomes to environmental conditions. It is possible to use the Leonard Model to predict the outcomes of multiple interacting populations, but pairwise competitive outcomes do not always scale to community-level performance [34–36]. When extending the model to more than two populations, the fundamental assumption is that the population with the highest performance value will dominate. This assumption is most likely to hold in communities with relatively few successful competitive strategies, leading to trait underdispersion, low species diversity and/or competitive hierarchies among individuals [6,37,38]. For example, forest fire frequency can select against tree species with thin bark [39], and persistent wind and cold can select against taller plants with high leaf area [40]. By further limiting the scope of inference to intraspecific or intra-guild competition, the model may still be useful even when niche differentiation and limiting similarity promote competitive intransitivity, trait diversity and divergent life-history strategies across functional guilds.

The Leonard Model is intentionally simple, easily scaling to encompass multiple environmental conditions. A critical assumption, however, is that 'Liebig's Law of the Minimum' [24] holds across these gradients (equations (2.2)–(2.3)). This law has been applied in various plant, animal and microbial systems [25,41,42], but its usefulness as the dominant framework for understanding and modelling nutrient co-limitation has been called into question [42,43]. Microbes can exhibit strong stoichiometric constraints [44,45], suggesting that our model may be particularly suited to investigating biotic interactions in these communities; yet caution should be taken when inferring community-level outcomes from individual-level nutrient requirements [42,46]. Furthermore, the model assumes constant environmental conditions, making it ideally suited for studies in

relatively homogeneous conditions (e.g. aquatic communities), or where performance correlates with broad-scale regional variables (e.g. dominance of gymnosperms over angiosperms in cold or dry habitats [47]). In highly heterogeneous environments, average ΔR may still relate to relative abundances or relative occurrences of species across the landscape, but it may not indicate areas of competitive exclusion. Indeed, environmental heterogeneity is often noted as a mechanism by which otherwise inferior competitors persist across a landscape [48].

Since the model makes no assumptions about the mechanism of competition, it naturally extends to those settings where competitive outcomes are mediated through interference or apparent competition. In some fungi and plants, for example, competitive dominance depends on the production of antagonistic secondary chemicals that protect against herbivory or limit growth and productivity of competitors [49–51]. In such settings, metabolite or toxin production may replace growth rate as the best performance metric to predict regions of competitive dominance and coexistence across environmental gradients. The flexibility of our modelling approach is furthered by the equality among the Monod function, the Michaelis–Menton kinetics equation and the Holling Type II functional response curve. In situations where the competitive outcome does not follow a functional form similar to those in figure 1, simple alterations to the model code should allow for alternative performance curves that are neither monotonic increasing nor saturating.

A remaining challenge is the identification of a single performance metric that reliably predicts competitive outcomes across multiple environmental conditions. Here, the use of isogenic strains competing through resource capture in tightly controlled nutrient conditions was selected so that competitive ability was likely directly proportional to growth rate [27], and thus the performance metric was anticipated. When the mechanism of competition is unknown, our modelling framework provides a quantitative means for testing, exploring and validating a causal link between candidate competitive response traits and competitive outcomes. A combined approach that uses our model in tandem with correlative niche models may provide a means of overcoming the limitations of each [12,16,52], facilitating causal inferences from otherwise correlative observations.

Although not a primary goal of our research, the use of isogenic and descendent strains shows that the model can identify trait evolution and corresponding competitive differences among closely related populations. Under carbon and nitrogen limitation, both descendent populations showed adaptation, but in ways that were somewhat counter to expectations based on resource limitation [30]. In particular, the Low-N evolved strain displayed a lower C_C value than the Low-C strain, making it more competitive at low carbon values as well as low nitrogen values. Although seemingly counterintuitive, this result could be owing to pleiotropy, such that mutations at some genes affect C_C, C_N and R_K [53]. An alternative, and perhaps more likely possibility is that the evolved Low-C strain adapted to both low carbon levels and also to other aspects of the chemostat environment, such as temperature (30°C), the constant aerobic environment, and/or pH (held at 6.0 ± 0.1). Certainly, a change in gene expression may have occurred when subject to the chemostat environment for many generations [54]. Regardless of the cause of the trait microevolution, our combined model and empirical data demonstrate an approach for linking trait variation to performance among closely related populations.

5. Conclusion

We provide a trait-based model that robustly predicts individual performance and competitive outcomes across an entire Hutchinsonian two-dimensional environmental gradient. The Leonard Model is most suited to those settings where competitive ability differs across environmental gradients, or where species compete through resource capture, interference, or apparent competition. When investigating genetically related or co-occurring species, our approach can be used to identify which traits result in competitive advantages. The theoretical and mathematical framework presented here provides a novel and generalizable method of modelling, predicting and visualizing the fundamental niche space and competitive outcomes using a strictly trait-based approach. Our work demonstrates the potential to link organismal traits directly to population-level outcomes across varying abiotic and biotic contexts, such as those occurring under environmental change.

Data accessibility. The datasets supporting this article have been uploaded as part of the electronic supplementary material.

Authors' contributions. D.S.M. wrote the manuscript with contributions from all authors. M.A.B. and K.E.L. designed and implemented the chemostat experiments. K.E.L. constructed the mathematical model. D.S.M., K.E.L., M.A.B. and T.W.C. analysed and interpreted the data. J.M.D. and D.W.H. assisted with design, implementation and analysis throughout.

Competing interests. The authors have no competing interests.

Funding. The work was supported by a faculty research grant for creative scholarship from the University of Georgia to M.A.B.

Acknowledgement. Data were collected and the model was originally developed by Ken E. Leonard for his doctoral research. They are reported here posthumously. We thank his family for their support of him in his studies and in the publication of this research. The yeast strains were provided by Mat Goddard.

References

1. Kissling WD *et al.* 2012 Towards novel approaches to modelling biotic interactions in multispecies assemblages at large spatial extents. *J. Biogeogr.* **39**, 2163–2178. (doi:10.1111/j.1365-2699.2011.02663.x)
2. Van der Putten WH, Macel M, Visser ME. 2010 Predicting species distribution and abundance responses to climate change: why it is essential to include biotic interactions across trophic levels. *Phil. Trans. R. Soc. B* **365**, 2025–2034. (doi:10.1098/rstb.2010.0037)
3. Zarnetske PL, Skelly DK, Urban MC. 2012 Biotic multipliers of climate change. *Science* **336**, 1516–1518. (doi:10.1126/science.1222732)
4. Violle C, Navas M-L, Vile D, Kazakou E, Fortunel C, Hummel I, Garnier E. 2007 Let the concept of trait be functional! *Oikos* **116**, 882–892. (doi:10.1111/j.2007.0030-1299.15559.x)
5. McGill BJ, Enquist BJ, Weiher E, Westoby M. 2006 Rebuilding community ecology from functional traits. *Trends Ecol. Evol.* **21**, 178–185. (doi:10.1016/j.tree.2006.02.002)
6. Crowther TW, Maynard D, Crowther T, Peccia J, Smith J, Bradford M. 2014 Untangling the fungal

niche: the trait-based approach. *Front. Microbiol.* **5**, 579. (doi:10.3389/fmicb.2014.00579)

7. Navas M-L, Moreau-Richard J. 2005 Can traits predict the competitive response of herbaceous Mediterranean species? *Acta Oecologica* **27**, 107–114. (doi:10.1016/j.actao.2004.10.002)
8. Schamp B, Chau J, Aarssen L. 2008 Dispersion of traits related to competitive ability in an old-field plant community. *J. Ecol.* **96**, 204–212. (doi:10.1111/j.1365-2745.2007.0)
9. Fynn RWS, Morris CD, Kirkman KP. 2005 Plant strategies and trait trade-offs influence trends in competitive ability along gradients of soil fertility and disturbance. **93**, 384–394. (doi:10.1111/j.0022-0477.2005.00993.x)
10. Gaudet CL, Keddy PA. 1988 A comparative approach to predicting competitive ability from plant traits. *Nature* **334**, 242–243. (doi:10.1038/334242a0)
11. Shipley B, Vile D, Garnier E. 2006 From plant traits to plant communities: a statistical mechanistic approach to biodiversity. *Science* **314**, 812–814. (doi:10.1126/science.1131344)
12. Kearney M, Porter W. 2009 Mechanistic niche modelling: combining physiological and spatial data to predict species' ranges. *Ecol. Lett.* **12**, 334–350. (doi:10.1111/j.1461-0248.2008.01277.x)
13. Kearney MR, Wintle BA, Porter WP. 2010 Correlative and mechanistic models of species distribution provide congruent forecasts under climate change. *Conserv. Lett.* **3**, 203–213. (doi:10.1111/j.1755-263X.2010.00097.x)
14. Laughlin DC, Joshi C, van Bodegom PM, Bastow ZA, Fulé PZ. 2012 A predictive model of community assembly that incorporates intraspecific trait variation. *Ecol. Lett.* **15**, 1291–1299. (doi:10.1111/j.1461-0248.2012.01852.x)
15. Soberon J, Peterson A. 2005 Interpretation of models of fundamental ecological niches and species' distributional areas. *Biodivers. Inf.* **2**, 1–10.
16. Buckley LB, Urban MC, Angilletta MJ, Crozier LG, Rissler LJ, Sears MW. 2010 Can mechanism inform species' distribution models? *Ecol. Lett.* **13**, 1041–1054. (doi:10.1111/j.1461-0248.2010.01479.x)
17. Kearney M, Simpson SJ, Raubenheimer D, Helmuth B. 2010 Modelling the ecological niche from functional traits. *Phil. Trans. R. Soc. B* **365**, 3469–3483. (doi:10.1098/rstb.2010.0034)
18. Tilman D. 1980 A graphical-mechanistic approach to competition and predation. *Am. Nat.* **116**, 362–393. (doi:10.1086/283633)
19. Tilman GD. 1984 Plant dominance along an experimental nutrient gradient. *Ecology* **65**, 1445–1453. (doi:10.2307/1939125)
20. Tilman D. 1985 The resource-ratio hypothesis of plant succession. *Am. Nat.* **125**, 827–852. (doi:10.1086/284382)
21. Miller TE, Burns JH, Munguia P, Walters EL, Kneitel JM, Richards PM, Mouquet N, Buckley HL. 2005 A critical review of twenty years' use of the resource-ratio theory. *Am. Nat.* **165**, 439–448. (doi:10.1086/428681)
22. Hutchinson GE. 1957 Concluding remarks. *Cold Spring Harb. Symp. Quant. Biol.* **22**, 415–427. (doi:10.1101/SQB.1957.022.01.039)
23. Monod J. 1949 The growth of bacterial cultures. *Annu. Rev. Microbiol.* **3**, 371–394. (doi:10.1146/annurev.mi.03.100149.002103)
24. Von Liebig J. 1840 *Die organische Chemie in ihrer Anwendung auf Agricultur und Physiologie*. Braunschweig, Germany: Vieweg.
25. Zinn M, Witholt B, Egli T. 2004 Dual nutrient limited growth: models, experimental observations, and applications. *J. Biotechnol.* **113**, 263–279. (doi:10.1016/j.jbiotec.2004.03.030)
26. Tilman D. 1977 Resource competition between plankton algae: an experimental and theoretical approach. *Ecology* **58**, 338–348. (doi:10.2307/1935608)
27. Dykhuizen DE, Hartl DL. 1983 Selection in chemostats. *Microbiol. Rev.* **47**, 150–168.
28. Holling CS. 1959 Some characteristics of simple types of predation and parasitism. *Can. Entomol.* **91**, 385–398. (doi:10.4039/Ent91385-7)
29. Michaelis L, Menten ML. 1913 Die Kinetik der Invertinwirkung. *Biochem Z* **49**, 333–369.
30. Goddard MR, Bradford MA. 2003 The adaptive response of a natural microbial population to carbon- and nitrogen-limitation. *Ecol. Lett.* **6**, 594–598. (doi:10.1046/j.1461-0248.2003.00478.x)
31. Dean AM, Thornton JW. 2007 Mechanistic approaches to the study of evolution: the functional synthesis. *Nat. Rev. Genet.* **8**, 675–688. (doi:10.1038/nrg2160)
32. Tilman D. 1986 Nitrogen-limited growth in plants from different successional stages. *Ecology* **67**, 555–563. (doi:10.2307/1938598)
33. Kramer AM, Drake JM. 2014 Time to competitive exclusion. *Ecosphere* **5**, 1–16. (doi:10.1890/ES14-00054.1)
34. Bennett JA, Lamb EG, Hall JC, Cardinal-McTeague WM, Cahill JF. 2013 Increased competition does not lead to increased phylogenetic overdispersion in a native grassland. *Ecol. Lett.* **16**, 1168–1176. (doi:10.1111/ele.12153)
35. Laird RA, Schamp BS. 2006 Competitive intransitivity promotes species coexistence. *Am. Nat.* **168**, 182–193. (doi:10.1086/506259)
36. Keddy PA, Shipley B. 1989 Competitive hierarchies in herbaceous plant communities. *Oikos* **54**, 234–241. (doi:10.2307/3565272)
37. Weiher E, Keddy P. 1995 Assembly rules, null models, and trait dispersion: new questions from old patterns. *Oikos* **74**, 159–164. (doi:10.2307/3545686)
38. Herben T, Goldberg DE. 2014 Community assembly by limiting similarity vs. competitive hierarchies: testing the consequences of dispersion of individual traits. *J. Ecol.* **102**, 156–166. (doi:10.1111/1365-2745.12181)
39. Cavender-Bares J, Kitajima K, Bazzaz FA. 2004 Multiple trait associations in relation to habitat differentiation among 17 Floridian oak species. *Ecol. Monogr.* **74**, 635–662. (doi:10.1890/03-4007)
40. Spasojevic MJ, Suding KN. 2012 Inferring community assembly mechanisms from functional diversity patterns: the importance of multiple assembly processes. *J. Ecol.* **100**, 652–661. (doi:10.1111/j.1365-2745.2011.01945.x)
41. Austin M. 2007 Species distribution models and ecological theory: a critical assessment and some possible new approaches. *Ecol. Model.* **200**, 1–19. (doi:10.1016/j.ecolmodel.2006.07.005)
42. Danger M, Daufresne T, Lucas F, Pissard S, Lacroix G. 2008 Does Liebig's law of the minimum scale up from species to communities? *Oikos* **117**, 1741–1751. (doi:10.1111/j.1600-0706.2008.16793.x)
43. Harpole WS *et al*. 2011 Nutrient co-limitation of primary producer communities. *Ecol. Lett.* **14**, 852–862. (doi:10.1111/j.1461-0248.2011.01651.x)
44. Cleveland CC, Liptzin D. 2007 C:N:P stoichiometry in soil: is there a 'Redfield ratio' for the microbial biomass? *Biogeochemistry* **85**, 235–252. (doi:10.1007/s10533-007-9132-0)
45. Sinsabaugh RL *et al*. 2008 Stoichiometry of soil enzyme activity at global scale. *Ecol. Lett.* **11**, 1252–1264. (doi:10.1111/j.1461-0248.2008.01245.x)
46. Kaiser C, Franklin O, Dieckmann U, Richter A. 2014 Microbial community dynamics alleviate stoichiometric constraints during litter decay. *Ecol. Lett.* **17**, 680–690. (doi:10.1111/ele.12269)
47. Augusto L, Davies TJ, Delzon S, De Schrijver A. 2014 The enigma of the rise of angiosperms: can we untie the knot? *Ecol. Lett.* **17**, 1326–1338. (doi:10.1111/ele.12323)
48. Tilman D, Pacala SW. 1993 *The maintenance of species richness in plant communities*. Chicago, IL: University of Chicago Press.
49. Crowther TW, Boddy L, Jones TH. 2011 Outcomes of fungal interactions are determined by soil invertebrate grazers. *Ecol. Lett.* **14**, 1134–1142. (doi:10.1111/j.1461-0248.2011.01682.x)
50. Sampedro L, Moreira X, Zas R. 2011 Costs of constitutive and herbivore-induced chemical defences in pine trees emerge only under low nutrient availability. *J. Ecol.* **99**, 818–827. (doi:10.1111/j.1365-2745.2011.01814.x)
51. Callaway R, Cipollini D, Barto K. 2008 Novel weapons: invasive plant suppresses fungal mutualists in America but not in its native Europe. *Ecology* **89**, 1043–1055. (doi:10.1890/07-0370.1)
52. Laughlin DC. 2014 Applying trait-based models to achieve functional targets for theory-driven ecological restoration. *Ecol. Lett.* **17**, 771–784. (doi:10.1111/ele.12288)
53. DeWitt T, Sih A, Wilson D. 1998 Costs and limits of phenotypic plasticity. *Trends Ecol. Evol.* **5347**, 77–81. (doi:10.1016/S0169)
54. Ferea TL, Botstein D, Brown PO, Rosenzweig RF. 1999 Systematic changes in gene expression patterns following adaptive evolution in yeast. *Proc. Natl Acad. Sci. USA* **96**, 9721–9726. (doi:10.1073/pnas.96.17.9721)